

# On optimal sensor placement and motion coordination for target tracking

Sulema Aranda Sonia Martínez Francesco Bullo  
 Mechanical and Environmental Engineering  
 University of California at Santa Barbara  
 Santa Barbara, CA, 93106-5070, USA  
 {smartine,bullo}@engineering.ucsb.edu

**Index Terms**—motion coordination, optimal sensor placement, Fisher Information Matrix, Kalman filtering.

**Abstract**—This work studies optimal sensor placement and motion coordination strategies for mobile sensor networks. For a target tracking application with range sensors, we investigate the determinant of the Cramer Rao Lower Bound and compute it in the 2D and 3D cases, characterizing the global minima in the 2D case. We propose motion coordination algorithms that steer the mobile sensor network to an optimal deployment and that are amenable to a decentralized implementation. Finally, our numerical simulations illustrate how the proposed algorithms lead to improved performance of an extended Kalman filter in a target tracking scenario.

## I. INTRODUCTION

New advancements in the fields of microelectronics and miniaturization have generated a tremendous surge of activity in the development of sensor networks. The envisioned groups of agents are endowed with communication, sensing and computation capabilities, and promise great efficiency in the realization of multiple tasks such as environmental monitoring, exploratory missions and search and rescue operations. However, several fundamental problems need to be solved in order to make this technology possible. One main difficulty is the requirement for decentralized architectures where each agent takes autonomous decisions based on information shared with only a few local neighbors. Ongoing research work focuses on decentralized filters and data-fusing methods for estimation, and on the motion algorithms that guarantee the desired global behavior of the network. Ideally, both the motion control algorithms and estimation processes should be optimally integrated to make the most of the network performance.

In this paper we investigate the design of distributed motion coordination algorithms that increase the information gathered by a network in static and dynamic target-tracking scenarios. To do this, we define an aggregate cost function encoding a “sensitivity performance measure” and design our algorithms to maximize it. This idea has been widely used in papers on optimum experimental design for dynamical systems with applications to measurement problems. An incomplete list of references is [3, 7, 11, 14]. For example [11, 14] deal with problems on target tracking and parameter identification of distributed parameter systems. The motion control algorithms proposed in these papers either are computed via some off-line numerical method or are gradient algorithms. Often these algorithms are designed to maximize an appropriate scalar

cost function and to choose the best sensor locations from a grid of finite candidates. Unfortunately, these schemes turn out to be not distributed since in order to define the control law for each agent, it is necessary to know all other agents’ positions at each step. A second set of relevant references are those on distributed motion coordination. Our proposed control algorithms are in the same spirit as those for cyclic pursuit [8], flocking [6], and coverage control [4].

The contributions of this paper are the following. Under the assumption of Gaussian noise measurements with diagonal correlation, Section II presents closed-form expressions for the determinant of the Fisher Information Matrix for “range-measurement” models in non-random static scenarios, for 2 and 3 dimensional state spaces. This determinant plays the role of an objective function: we characterize its critical points in the 2D version and obtain sets of positions that globally maximize its value. If the sensors measure distances to the target, then an optimal configuration is one in which the sensors are uniformly placed in circular fashion around the target, confirming a natural intuition about the problem. Taking this optimal configuration as a starting point in Section III, we then consider a target tracking scenario where the sensors move along the boundary of a convex set containing the target. We define discrete-time control laws that, relying only on local information, achieve the uniform configuration around the target (estimate) exponentially fast. In essence, our laws are very intuitive and simple-to-implement interaction behaviors between the sensors along the boundary. Finally, in Section IV, we numerically validate our coordination and optimal deployment laws in a particular dynamic target-tracking scenario. Although the network achieves global optimum configurations for a *nonrandom static* parameter estimation scenario, we simulate a *dynamic random* scenario. Our simulations illustrate the following reasonable conjecture: optimizing the sensitivity function for the static non-random case improves the performance of a filter (in our case an EKF) for the dynamic random scenario.

Finally, we point out that we assume that the process of estimation is performed by a central site or by a distributed process that we do not implement here. For works dealing with multisensor fusion possibly under communication constraints we refer to [5, 10, 12, 13] and references therein.

## II. OPTIMAL PLACEMENT OF SENSORS

Here we present the assumptions on our sensor network and target models in (1) (non-random) static estimation scenarios

and (2) (random) dynamic parameter estimation scenarios. We obtain the corresponding Fisher Information Matrices (FIMs) and analyze the global minima of their determinant as a means to guarantee increased sensitivity with respect to the sensors' measurements. See [2] for a comprehensive treatment on estimation and tracking.

#### A. The static parameter estimation scenario

The localization of static targets can be solved as a non-random parameter estimation problem as follows. Let  $p_j \in \mathbb{R}^d$ ,  $j \in \{1, \dots, n\}$ , denote the position of  $n$  sensors moving in a convex region  $Q \subseteq \mathbb{R}^d$  and let  $q_0 \in Q$  be the unknown target position to be estimated by means of the measurement model:

$$z_j(q) = h(\|q - p_j\|) + w_j, \quad q \in Q, \quad (1)$$

for  $j \in \{1, \dots, n\}$ . Here,  $h : [0, +\infty) = \mathbb{R}_+ \rightarrow \mathbb{R}$  is defined according to the particular sensors' specifications and  $w_j$  represents a white noise,  $j \in \{1, \dots, n\}$ . The stacked vector of measurements at a given instant is a random vector normally distributed as

$$Z \triangleq \begin{bmatrix} z_1 \\ \vdots \\ z_n \end{bmatrix} \sim \mathcal{N} \left( \begin{bmatrix} h(\|q - p_1\|) \\ \vdots \\ h(\|q - p_n\|) \end{bmatrix}, R \right),$$

where  $R = R^T > 0$  is the  $n \times n$  covariance matrix. From now on, we will use the shorthand notation  $Z = (z_1, \dots, z_n)^T$ , and  $H$  will denote the function  $H(q, p_1, \dots, p_n) = (h(\|q - p_1\|), \dots, h(\|q - p_n\|))^T$ .

The *Fisher Information Matrix* (FIM) for non-random parameters, denoted by  $J_{\text{NR}}$ , is defined as the expected value with respect to the probability distribution  $p(Z|q)$ :

$$J_{\text{NR}} \triangleq E \left[ (\nabla_q \log \Lambda) \cdot (\nabla_q \log \Lambda)^T \right]_{q=q_0},$$

where  $q_0$  is the true value of the target location or an estimate of it,  $\nabla_q = (\frac{\partial}{\partial q^1}, \dots, \frac{\partial}{\partial q^d})^T$ , and  $\Lambda$  is the *likelihood function*,

$$\Lambda(q, p_1, \dots, p_n) = \frac{1}{\sqrt{2\pi \det R}} \exp \left( -\frac{1}{2} (Z - H)^T R^{-1} (Z - H) \right).$$

A few computations show  $J_{\text{NR}} = (\nabla_q H)_{q_0}^T R^{-1} (\nabla_q H)_{q_0}$ . Let  $q = (q^1, \dots, q^d)^T$ , and define the shorthands

$$\partial_\ell h_j(q_0, p_1, \dots, p_n) \triangleq \frac{\partial}{\partial q^\ell} h(\|q - p_j\|) \Big|_{q=q_0},$$

for  $j \in \{1, \dots, n\}$  and  $\ell \in \{1, \dots, d\}$ . Then  $(\nabla_q H)_{q_0} : \mathbb{R}^d \times (\mathbb{R}^n)^d \rightarrow \mathbb{R}^{n \times n}$  can be computed to be

$$((\nabla_q H)_{q_0})_{j\ell}(q_0, p_1, \dots, p_n) = \partial_\ell h_j(q_0, p_1, \dots, p_n),$$

for  $j \in \{1, \dots, n\}$  and  $\ell \in \{1, \dots, d\}$ . In the particular case that  $R = \sigma^2 I_n$ , the FIM  $J_{\text{NR}}$  can be expressed as:

$$J_{\text{NR}}(q_0, p_1, \dots, p_n) = \frac{1}{\sigma^2} (\nabla_q H)_{q_0}^T (\nabla_q H)_{q_0} = \frac{1}{\sigma^2} \sum_{j=1}^n \begin{bmatrix} (\partial_1 h_j)^2 & \dots & (\partial_1 h_j)(\partial_d h_j) \\ \vdots & \ddots & \vdots \\ (\partial_d h_j)(\partial_1 h_j) & \dots & (\partial_d h_j)^2 \end{bmatrix}. \quad (2)$$

#### B. The dynamic parameter estimation scenario

Dynamic targets can be thought of as random parameters evolving under a stochastic difference equation. Here we assume that the target position  $q(k)$ , at time  $k \in \mathbb{N} \cup \{0\}$  satisfies:

$$q(k) = F_k(q(k-1)) + v(k), \quad k \geq 1, \quad q(0) \in Q,$$

for some functions  $F_k : \mathbb{R}^d \rightarrow \mathbb{R}^d$  and  $v(k)$  i.i.d as  $v(k) \sim \mathcal{N}(0, N(k))$ , where  $N(k) = N(k)^T > 0$ , for  $k \geq 0$ , and  $E[v(k_1)v(k_2)^T] = \delta_{12}N(k_1)$ , for  $k_1, k_2 \geq 0$ . Similarly as before, we model our sensor network as

$$Z(k) = H_k(q(k), p_1(k), \dots, p_n(k)) + w(k), \quad k \geq 0,$$

with  $H_k(q(k), p_1(k), \dots, p_n(k)) = (h_k(\|q(k) - p_1(k)\|), \dots, h_k(\|q(k) - p_n(k)\|))$ , where  $h_k : \mathbb{R}_+ \rightarrow \mathbb{R}$ , and  $Z(k) = (z_1(k), \dots, z_n(k))$ ,  $k \geq 0$ . We will assume that  $w(k) \sim \mathcal{N}(0, R(k))$ , where  $R(k) = R(k)^T > 0$ ,  $k \geq 0$ , and that  $E[w(k_1)w(k_2)^T] = \delta_{12}R(k_1)$ , for  $k_1, k_2 \geq 0$ .

An estimation method that is widely employed for target tracking is that of the Extended Kalman Filter (EKF) [2]. The assumptions for the filter require  $q(k)$  and  $Z(k)$  to be jointly Gaussian distributed with covariance  $P(k) = P(k)^T$ , and  $E[q(k_1)w(k_2)] = 0$ , for  $k_1, k_2 \geq 0$ . The EKF provides a state estimate  $q_e(k)$  together with an estimate for the covariance of the error  $P_e(k)$ :

$$P_e(k) = P_p(k) - W(k)S(k)W(k)^T, \quad k \geq 1,$$

where  $P_p(k)$  is the predicted covariance of the error and  $W(k)$ ,  $S(k)$  are some matrices appropriately defined [2]. Let  $q_p(k)$  be the predicted value of  $q(k)$ . Some standard computations [2, 10], allow us to say that

$$P_e^{-1}(k) = P_p^{-1}(k) + (\nabla_q H_{k|q_p(k)})^T R^{-1}(k) \nabla_q H_{k|q_p(k)}$$

or, denoting  $(\nabla_q H_{k|q_p(k)})^T R^{-1}(k) \nabla_q H_{k|q_p(k)} = J_{\text{NR}}(k)$ ,

$$P_e^{-1}(k) = P_p^{-1}(k) + J_{\text{NR}}(k), \quad k \geq 0. \quad (3)$$

Similarly, it can be seen that for linear measurement and linear target models, the FIM for dynamic (random) parameters,  $J_{\text{DR}}(k)$ , and  $J_{\text{NR}}(k)$  satisfy

$$J_{\text{DR}}(k) = J_{\text{NR}}(k) + J(k), \quad T(k) = T(k)^T \geq 0. \quad (4)$$

#### C. Cost functions for optimal sensing

As is well known, the FIM encodes the amount of information that a set of measurements produces in estimating a set of parameters. Under the assumptions made in former sections, we have  $\text{FIM} = \text{CRLB}^{-1}$ ; i.e., the FIM is the inverse of the Cramer Rao Lower Bound, which in turn lower bounds the covariance of the error<sup>1</sup>

$$\text{FIM}^{-1} = \text{CRLB} \leq E[(\hat{q} - q_0)(\hat{q} - q_0)^T].$$

Because of this, one expects that "minimizing the CRLB" results in a decrease of uncertainty.

This line of reasoning has been a main theme in several papers dealing with *optimum experimental design* and *active sensing*, e.g., see [11, 14]. Starting from the FIM (resp. the CRLB) of the estimation approach, an *evaluation*

<sup>1</sup>For efficient estimators, the inequality is an equality.

function is defined (usually the determinant or the trace of the FIM/CRLB) whose maximization (resp. its minimization) is to be achieved. For example, the det FIM is the cost function is ‘‘D-optimum design’’ as discussed by [14].

As before, let  $q_0 \in \mathbb{R}^d$  be the true value of the target location or an estimate of it. Under the assumptions of Subsection II-A and II-B, we define our cost function  $\mathcal{L}_{q_0} : (\mathbb{R}^d)^n \rightarrow \mathbb{R}_+$  by

$$\mathcal{L}_{q_0}(p_1, \dots, p_n) = \det J_{\text{NR}}(q_0, p_1, \dots, p_n), \quad (5)$$

with  $J_{\text{NR}}$  given in (2). Because of (3) and (4), we are guaranteed that, if we optimize  $\mathcal{L}_{q_0}$  with respect to the positions of the sensors, then we will get increased performance in static estimation scenarios, and expect reasonably good performance in dynamic ones.

In what follows we derive the expression for the cost function  $\mathcal{L}_{q_0}$  for  $d = 2$  and  $d = 3$  and analyze its critical points and global maxima. To do this, we shall assume that our measurement model is

$$h(r) = \begin{cases} (r - c_1)^b + c_2, & R_0 < r < R_1, \\ 0, & \text{otherwise,} \end{cases} \quad (6)$$

for  $b \in \mathbb{Z}$ , and constants  $R_1 > R_0 > 0$ ,  $c_2, c_1 \in \mathbb{R}_+$ . Range sensors such as sonars can be modeled by  $b = 1$  and  $c_1 = c_2 = 0$ .

*Proposition 2.1:* For  $q_0 \in \mathbb{R}^d$ , let  $\mathcal{L}_{q_0} : (\mathbb{R}^d)^n \rightarrow \mathbb{R}_+$  be defined as in (5) and  $h$  be defined as in (6). Let  $\mathcal{S}_{q_0}(p_1, \dots, p_n)$  be the set of indices  $i \in \{1, \dots, n\}$  such that  $R_0 < \|p_i - q_0\| < R_1$ . The following statements hold true.

(i) For  $d = 2$ ,

$$\mathcal{L}_{q_0}(p_1, \dots, p_n) = \frac{1}{2\sigma^2} \sum_{i,j \in \mathcal{S}_{q_0}} \|\mathbf{v}_i\|^2 \|\mathbf{v}_j\|^2 \sin^2 \alpha_{ij}$$

where  $\alpha_{ij} \triangleq \angle(\mathbf{v}_i, \mathbf{v}_j)$ ,  $\mathbf{v}_i = (\partial_1 h_i, \partial_2 h_i, 0)$ , and  $\|\mathbf{v}_i\|^2 = b^2(\|p_i - q_0\| - c_1)^{2(b-1)}$ , for  $i, j \in \mathcal{S}_{q_0}(p_1, \dots, p_n)$ .

(ii) For  $d = 3$ ,

$$\mathcal{L}_{q_0}(p_1, \dots, p_n) = \frac{1}{6\sigma^2} \sum_{i,j,k \in \mathcal{S}_{q_0}} \|\mathbf{v}_i\|^2 \|\mathbf{v}_j\|^2 \|\mathbf{v}_k\|^2 \sin^2 \alpha_{ij} \cos^2 \beta_{ij,k}$$

where  $\alpha_{ij} \triangleq \angle(\mathbf{v}_i, \mathbf{v}_j)$ ,  $\beta_{ij,k} \triangleq \angle(\mathbf{v}_i \times \mathbf{v}_j, \mathbf{v}_k)$ , and  $\mathbf{v}_i = (\partial_1 h_i, \partial_2 h_i, \partial_3 h_i)$ , with  $\|\mathbf{v}_i\|^2 = b^2(\|p_i - q_0\| - c_1)^{2(b-1)}$ , for  $i, j, k \in \mathcal{S}_{q_0}(p_1, \dots, p_n)$ .

Here we understand that  $\mathcal{L}_{q_0} = 0$  when  $\mathcal{S}_{q_0} = \emptyset$ .

The proof of this result is in [1].

Let us now introduce some useful notation. Let  $\mathbb{T}$  be the circle in the plane and define  $\mathcal{L}_{\mathbb{T}} : \mathbb{T}^n \rightarrow \mathbb{R}_+$  by

$$\mathcal{L}_{\mathbb{T}}(\delta_1, \dots, \delta_n) = \frac{b^4 M^2}{2\sigma^2} \sum_{i,j \in \{1, \dots, n\}} \sin^2(\delta_i - \delta_j),$$

where  $M = \max_{r \in [R_0, R_1]} (r - c_1)^{2(b-1)} > 0$ . Now, let  $d = 2$  and assume  $q_0 \neq p_i$ , for  $i \in \{1, \dots, n\}$ . Consider a polar change of coordinates centered at  $q_0 \in \mathbb{R}^2$ , and identify  $p_i \in \mathbb{R}^2$  with  $(\eta_i, r_i)$  for some  $\eta_i \in \mathbb{T}$  and  $r_i \in \mathbb{R}_+$ ,  $i \in \{1, \dots, n\}$ . We then have that  $\mathcal{L}_{q_0}(p_1, \dots, p_n) \leq \mathcal{L}_{\mathbb{T}}(\eta_1, \dots, \eta_n)$  and  $(p_1, \dots, p_n)$  is a global maximum of  $\mathcal{L}_{q_0}$  if and only if

$(\eta_1, \dots, \eta_n)$  is a global maximum of  $\mathcal{L}_{\mathbb{T}}$  and  $(r_i - c_1)^{2(b-1)} = M$ , for all  $i \in \{1, \dots, n\}$ . We now analyze the maxima of  $\mathcal{L}_{\mathbb{T}}$ .

*Proposition 2.2:* The following statements hold true.

(i) The point  $(\eta_1, \dots, \eta_n) \in \mathbb{T}^n$  is a critical point for  $\mathcal{L}_{\mathbb{T}}$  if either any two vectors in  $\{(\cos 2\eta_i, \sin 2\eta_i)\}_{i=1}^n$  are aligned or

$$\sum_{i \in \{1, \dots, n\}} \cos 2\eta_i = 0, \text{ and } \sum_{i \in \{1, \dots, n\}} \sin 2\eta_i = 0,$$

(ii) The following three quantities are equal:  $\frac{b^4 M^2}{4\sigma^2} n$ ,  $\max \{\mathcal{L}_{q_0}(p_1, \dots, p_n) \mid p_1, \dots, p_n \in \mathbb{R}^d\}$ , and  $\max \{\mathcal{L}_{\mathbb{T}}(\delta_1, \dots, \delta_n) \mid \delta_1, \dots, \delta_n \in \mathbb{T}\}$ .

(iii) If  $\eta_i = (i - 1)\pi/n$ ,  $i \in \{1, \dots, n\}$ , then

$$\{(\eta_1 + k_1\pi, \dots, \eta_n + k_n\pi) \mid k_1, \dots, k_n \in \mathbb{Z}\}$$

are global maxima for  $\mathcal{L}_{\mathbb{T}}$ .

The proof of this result is in [1].

*Remark 2.3:* By (iii) there could be global maxima with multiple sensors at the same position. This could be a consequence of our assumptions that the measurement noises  $w_j$  are uncorrelated. It is a conjecture that, if the  $w_j$  depended on the sensors locations, then coincident locations could not be part of the set of maximum points. •

### III. DECENTRALIZED MOTION COORDINATION FOR THE NON-RANDOM PARAMETER SCENARIO

This section presents a family of decentralized control laws that steers the sensors to a set of points of maximum for the cost functions previously defined. Our analysis is related to the approaches in [4, 6, 8]. We make the following assumptions on the agents’ motion, sensing, and communication:

- (i) a static target  $q_0$  takes values in the interior of a compact convex set  $Q$  with boundary  $\partial Q$ ;
- (ii) the measurement model is the one described in equation (1) with  $h(r) = r$ , i.e., equation (6) with  $\gamma = 1$ ,  $b = 1$ ,  $c_1 = c_2 = 0$ ,  $R_0 = 0$ ,  $R_1 = +\infty$ ;
- (iii) each of the sensors  $\{p_1, \dots, p_n\}$  moves in discrete time along  $\partial Q$ ;
- (iv) each of the sensors  $\{p_1, \dots, p_n\}$  detects its immediate clockwise and counterclockwise neighbors in  $\partial Q$  and acquires the corresponding distances.

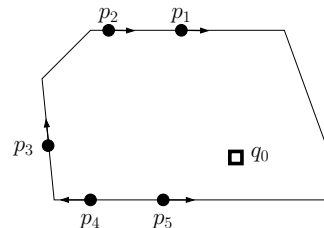


Fig. 1. Assumptions (i) and (iii): the sensors move along the boundary of  $Q$  and the target moves inside  $Q$ .

For this static scenario with limited information, the motion coordination objective is to steer  $\{p_1, \dots, p_n\}$  to the equally-spaced angular positions around the target  $q_0$  exponentially fast.

- Remark 3.1:*
- Assumption (iv) means that an implementable control law for an agent can only depend on the agent's position relative to its neighbors (in the natural ring topology along  $\partial Q$ ). We will call such a control law *spatially distributed along  $\partial Q$* .
  - We will allow the control law to depend on the current estimate of the target location. This strategy is said to be of the “certainty equivalence” type. •

### A. From the boundary of $Q$ to a circle and back

Because we assume that the  $n$  sensors can be placed only along  $\partial Q$ , we will work with the polar coordinates of  $\{p_1, \dots, p_n\}$  centered at  $q_0$  and define our motion control algorithms on the circle.

Let  $\partial Q$  be implicitly defined by the continuous equation  $x \in \partial Q$  if and only if  $g(x) = 0$ . Given a point  $q$  in the interior of a compact convex set  $Q$ , define the map  $\varphi_q : \partial Q \rightarrow \mathbb{T}$  by

$$\varphi_q(p) = \frac{p - q}{\|p - q\|}.$$

One can show that  $\varphi_q$  is continuous with continuous inverse  $\varphi_q^{-1} : \mathbb{T} \rightarrow \partial Q$  given by  $\varphi_q^{-1}(v) = q + \lambda v$  where  $\lambda \in \mathbb{R}_+$  the unique solution to  $g(q + \lambda p) = 0$ .

In what follows, we let  $q_0$  denote the current estimate of the target location, we let  $\varphi_{q_0}(p)$  be the angular component of the polar coordinates of  $p$  centered at  $q_0$ , and we identify  $p_i \in \partial Q \subset \mathbb{R}^2$  with  $\eta_i = \varphi_{q_0}(p_i) \in \mathbb{T}$ , for all  $i$ .

### B. Basic behaviors for uniform coverage of the circle

As discussed, the location of the sensors is described by the vector  $(\eta_1, \dots, \eta_n)$  of elements of  $\mathbb{T}$ . We assume that angles are measured counterclockwise and that the sensors are placed in counterclockwise order (we adopt the convention that  $\eta_{n+1} = \eta_1$  and that  $\eta_0 = \eta_n$ ).

As described Assumption (iii), the sensors motion is described by a discrete-time control system:

$$\eta_i(k+1) = \eta_i(k) + u_i, \quad i \in \{1, \dots, n\}.$$

Here  $u_i$  is the scalar control magnitude of the  $i$ th sensor. In a way consistent with Assumption (iv), we assume  $u_i$  is a function only of the relative angular distances in the counterclockwise direction  $d_{\text{counterclock},i} = \eta_{i+1} - \eta_i > 0$  and clockwise direction  $d_{\text{clock},i} = \eta_i - \eta_{i-1} > 0$ . We also assume that each sensor obeys the same motion control law  $u : [0, 2\pi] \times [0, 2\pi] \rightarrow \mathbb{R}$ , so that the closed-loop system becomes:

$$\begin{aligned} \eta_i(k+1) &= \eta_i(k) + u(d_{\text{counterclock},i}(k), d_{\text{clock},i}(k)), \\ d_{\text{counterclock},i}(k) &= \eta_{i+1}(k) - \eta_i(k), \\ d_{\text{clock},i}(k) &= \eta_i(k) - \eta_{i-1}(k). \end{aligned}$$

In order to achieve uniform distribution of the sensors on the circle, two simple behaviors arise fairly naturally, see Figure 2. First, we consider the GO TOWARDS THE MIDPOINT behavior with  $u_{\text{midpoint}} : [0, 2\pi] \times [0, 2\pi] \rightarrow \mathbb{R}$

$$u_{\text{midpoint}}(d_{\text{counterclock}}, d_{\text{clock}}) = \frac{1}{2}(d_{\text{counterclock}} - d_{\text{clock}}).$$

The interpretation is clear: each sensor moves towards the midpoint of the angular segment between the preceding and

following sensor. In the original coordinate system, each sensor moves along  $\partial Q$  towards the bisector of the triangle with vertex  $q_0$  and vertices given by the preceding and following sensor. A second intuitive rule is the GO TOWARDS THE

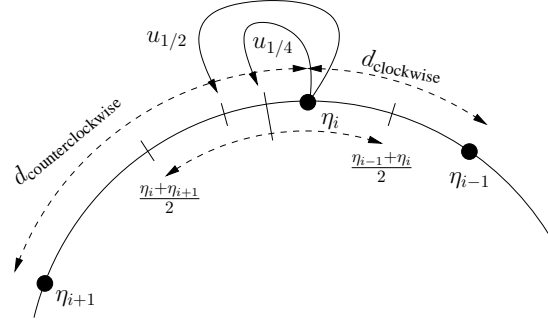


Fig. 2. The GO TOWARDS THE MIDPOINT  $u_{1/2}$  and GO TOWARDS THE MIDPOINT OF VORONOI SEGMENT  $u_{1/4}$  behaviors.

MIDPOINT OF VORONOI SEGMENT behavior  $u_{\text{midpoint Voronoi}} : [0, 2\pi] \times [0, 2\pi] \rightarrow \mathbb{R}$

$$u_{\text{midpoint Voronoi}}(d_{\text{counterclock}}, d_{\text{clock}}) = \frac{1}{4}(d_{\text{counterclock}} - d_{\text{clock}}).$$

The interpretation is the following: the Voronoi segment of the  $i$ th sensor at position  $\eta_i$  is the angular segment from  $(\eta_{i-1} + \eta_i)/2$  to  $(\eta_i + \eta_{i+1})/2$ , and the control law GO TOWARDS THE MIDPOINT OF VORONOI SEGMENT steers  $\eta_i$  towards the midpoint of this segment.

These two rules are particular instances of the following family of linear algorithms parametrized by  $\mathcal{K} \in \mathbb{R}$ :

$$u_{\mathcal{K}}(d_{\text{counterclock}}, d_{\text{clock}}) = \mathcal{K}(d_{\text{counterclock}} - d_{\text{clock}}).$$

Clearly,  $u_{\text{midpoint}}$  and  $u_{\text{midpoint Voronoi}}$  are equal to  $u_{\mathcal{K}}$  for  $\mathcal{K} = 1/2$  and  $\mathcal{K} = 1/4$ , respectively. Because  $u_{\mathcal{K}}(d, d) = 0$  for all  $d \in \mathbb{R}_+$ , the equally-spaced angle position (where the sensors are uniformly distributed around the target) is an equilibrium point<sup>2</sup> for the  $u_{\mathcal{K}}$ -closed-loop system.

### C. Convergence analysis

To perform a convergence analysis, it is convenient to define the relative angular distances  $d_i = \eta_{i+1} - \eta_i$ , for  $i \in \{1, \dots, n\}$  (and adopt the usual convention that  $d_{n+1} = d_1$  and that  $d_0 = d_n$ ). So long as the counterclockwise order of the sensors is not violated, we have  $(d_1, \dots, d_n) \in S_{2\pi} = \{x \in \mathbb{R}_n \mid x_i \geq 0, \sum_{i=1}^n x_i = 2\pi\}$ . The change of coordinates from  $(\eta_1, \dots, \eta_n)$  to  $(d_1, \dots, d_n)$  and the control law  $u_{\mathcal{K}}$  jointly lead to the closed-loop system

$$d_i(k+1) = \mathcal{K}d_{i+1}(k) + (1 - 2\mathcal{K})d_i(k) + \mathcal{K}d_{i-1}(k).$$

<sup>2</sup>The more general linear feedback  $u(d_{\text{counterclock}}, d_{\text{clock}}) = ad_{\text{counterclock}} + bd_{\text{clock}}$  does not have the desired equilibrium set unless  $a + b = 0$ . The case of  $a + b \neq 0$  is studied in the context of cyclic pursuit, e.g., see [8].

This is a linear time-invariant dynamical system with state  $d = (d_1, \dots, d_n)$ , transition matrix  $A_{\mathcal{K}}$  given by

$$\begin{bmatrix} 1-2\mathcal{K} & \mathcal{K} & 0 & \dots & 0 & \mathcal{K} \\ \mathcal{K} & 1-2\mathcal{K} & \mathcal{K} & \ddots & \ddots & 0 \\ 0 & \mathcal{K} & 1-2\mathcal{K} & \ddots & \ddots & \vdots \\ \vdots & \ddots & \ddots & \ddots & \ddots & 0 \\ 0 & \ddots & \ddots & \mathcal{K} & 1-2\mathcal{K} & \mathcal{K} \\ \mathcal{K} & 0 & \dots & 0 & \mathcal{K} & 1-2\mathcal{K} \end{bmatrix},$$

and governing equation

$$d(k+1) = A_{\mathcal{K}}d(k), \quad \text{for } k \in \mathbb{N} \cup \{0\}. \quad (7)$$

*Theorem 3.2:* The control law  $u_{\mathcal{K}}$  is spatially distributed along  $\partial Q$ , and, for  $\mathcal{K} \in ]0, 1/2[$ , the solutions to the corresponding closed-loop system (7) preserve the counterclockwise order of the sensors and converge exponentially fast to  $(2\pi/n, \dots, 2\pi/n)$ .

**Proof.** Recall the notion and properties of circulant matrices from [9]. Note that  $A_{\mathcal{K}}$  is circulant with representer  $p_{A_{\mathcal{K}}}(s) = (1-2\mathcal{K}) + \mathcal{K}s + \mathcal{K}s^{n-1}$ . This implies that the eigenvalues of  $A_{\mathcal{K}}$  are

$$\lambda_{\ell} = p_{A_{\mathcal{K}}}\left(\exp\left(\frac{2\pi\ell\sqrt{-1}}{n}\right)\right) = 1 - 2\mathcal{K} + 2\mathcal{K}\cos\left(\frac{2\pi\ell}{n}\right),$$

for  $\ell \in \{1, \dots, n\}$ . One can see that  $\lambda_n = 1$  with corresponding eigenvector  $\mathbf{1}^T = (1, \dots, 1)$ . If  $\mathcal{K} > 0$  and  $\ell \in \{1, \dots, n-1\}$ , then

$$-1 \leq \cos\left(\frac{2\pi\ell}{n}\right) < 1 \implies 1 - 4\mathcal{K} \leq \lambda_{\ell} < 1.$$

Therefore, if  $\mathcal{K} \in ]0, 1/2[$ , then the eigenvalues  $\lambda_1, \dots, \lambda_{n-1}$  belong to the interval  $] -1, 1[$ . Additionally, if  $\mathcal{K} \in ]0, 1/2[$ , then  $A_{\mathcal{K}}$  is a doubly-stochastic matrix, which implies that  $S_{2\pi}$  is invariant for  $A_{\mathcal{K}}$ .

Let  $\{\mathbf{e}_1, \dots, \mathbf{e}_{n-1}, \mathbf{1}\}$  be a basis of orthogonal eigenvectors for  $A_{\mathcal{K}}$  corresponding to the eigenvalues  $\{\lambda_1, \dots, \lambda_n\}$ , respectively. Any initial condition  $d(0)$  can be written as

$$d(0) = \sum_{\ell=1}^{n-1} \rho_{\ell} \mathbf{e}_{\ell} + \rho_n \mathbf{1}.$$

Since  $\sum_{i=1}^n d_i(0) = 2\pi$ , one can see that  $\rho_n = \frac{2\pi}{n}$ . Therefore

$$d(k) = A_{\mathcal{K}}d(k-1) = \sum_{\ell=1}^{n-1} \lambda_{\ell}^k \rho_{\ell} \mathbf{e}_{\ell} + \frac{2\pi}{n} \mathbf{1}.$$

If  $\mathcal{K} \in ]0, 1/2[$ , then each  $|\lambda_{\ell}| < 1$ , for  $\ell \in \{1, \dots, n-1\}$  and, therefore, each trajectory  $k \mapsto d(k)$  converges to  $\frac{2\pi}{n} \mathbf{1}$ , the equal-angle configuration, exponentially fast.

- Remark 3.3:*
- (i) The properties of  $u_{\mathcal{K}}$  in Theorem 3.2 are independent of the number  $n$  of sensors.
  - (ii) If  $\mathcal{K} < 0$  or  $\mathcal{K} > 1/2$ , then there exist initial conditions from which the counterclockwise order of the sensors is not preserved in the closed loop.
  - (iii) Consider the  $\mathcal{K} = 1/2$  case, corresponding to the GO TOWARDS THE MIDPOINT behavior. Although GO TOWARDS THE MIDPOINT is a very natural algorithm to consider, it does *not* ensure convergence to the desired configuration whenever  $n$  is even. In fact, if  $n = 2L$

with  $L \in \mathbb{Z}$ , then  $\mathbf{1}$  and  $\mathbf{e}_L^T = (-1, 1, -1, \dots, -1, 1)$  are eigenvectors with eigenvalues 1 and  $-1$  respectively. Given  $\{\mathbf{e}_1, \dots, \mathbf{e}_{n-1}, \mathbf{1}\}$  an orthogonal basis of eigenvectors for  $A_{1/2}$  and  $d(0) = \sum_{i=1}^{n-1} \rho_i \mathbf{e}_i + \rho_n \mathbf{1}$ , one can show that, starting from arbitrary initial conditions, the system will exponentially converge to a steady oscillation between  $\mathbf{u}_1 = \rho_n \mathbf{1} + \rho_L \mathbf{e}_L$  and  $\mathbf{u}_2 = \rho_n \mathbf{1} - \rho_L \mathbf{e}_L$ .

#### IV. TARGET TRACKING SIMULATIONS WITH KALMAN FILTERING AND MOTION COORDINATION ALGORITHMS

Here we combine the developments of former sections to define the Active Target Tracking algorithm for collective improved sensing performance. We numerically simulate the algorithm to validate our approach. It is assumed that the estimation step is carried out after a round of communication has taken place to propagate all the measurements taken among the agents<sup>3</sup>. The algorithm is summarized in the following table.

<b>Name:</b>	ACTIVE TARGET TRACKING ALGORITHM
<b>Goal:</b>	Decentralized motion coordination of sensors and joint localization of target
<b>Data:</b>	(i) Constant $\mathcal{K} \in ]0, 1/2[$ . (ii) Equation for the boundary of the containment region, $g(q) = 0$ . (iii) Guess for target initial position $\hat{q}_0(0)$ .

At time  $k$ , local agent  $i \in \{1, \dots, n\}$  performs:

- 1: Receive estimate  $\hat{q}_0(k)$  from fusion center.
- 2: Detect counterclockwise and clockwise neighbors along  $\partial Q$ , compute angular distances in polar coordinates about  $\hat{q}_0(k)$ .
- 3: Compute control  $u_{\mathcal{K}}$ , next desired position  $\eta_i(k+1) \in \mathbb{T}$ , and corresponding point  $p_i(k+1) \in \partial Q$ .
- 4: Move to new position  $p_i(k+1)$  along  $\partial Q$ .
- 5: Take new measurement of target  $z_i(k+1)$ , and send it to fusion center, that will update target estimate according to EKF.

In what follows we present our numerical results. we compare the estimation errors of the trajectory of a dynamic target obtained from a set of four stationary and moving sensors. For the purpose of the simulation,  $Q$  will be a ball centered at the origin with radius  $1.5m$ , and the trajectory or the target will be the eight-shaped curve:

$$\begin{bmatrix} q_0^1(k) \\ q_0^2(k) \end{bmatrix} = \begin{bmatrix} \sin(\omega k) \\ \sin(\omega k) \cos(\omega k) \end{bmatrix}, \quad k \geq 0.$$

Here  $(q_0^1, q_0^2)$  are measured in meters and  $\omega = .1$  rad/sec.

In all the subsequent figures, the plots compares the evolution of the absolute error trajectories along time,  $E(k) = \|q_0(k) - \hat{q}_0(k)\|$  for stationary sensors (solid blue line) and moving sensors (dashed red line), for  $k \geq 0$ .

The first set of simulations, Figure 3, reproduce the results obtained for four sensors initially positioned at 2.1818, 2.4500, 3.7160, and 4.5167 radians. As can be seen, the moving sensors perform better on average as the variance increases.

In the second set of simulations, Figure 4, we take as the initial position for the sensors the optimal position to estimate  $\mathbf{0}$ . That is,  $0, \pi/2, \pi$  and  $3\pi/2$ , are the initial positions for both stationary and moving sensors. Though the set of moving

<sup>3</sup>This would be equivalent as having a fusion center that centralizes the estimation process

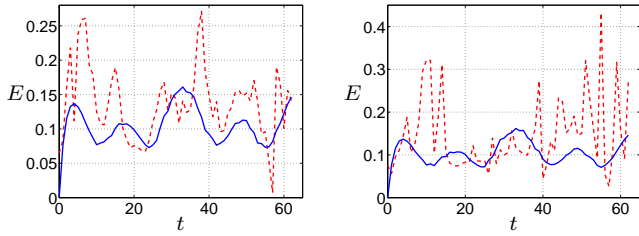


Fig. 3. Evolution of absolute error trajectories with variances of measured noise  $5 \times 10^{-3}$  (left) and  $5 \times 10^{-2}$  (right).

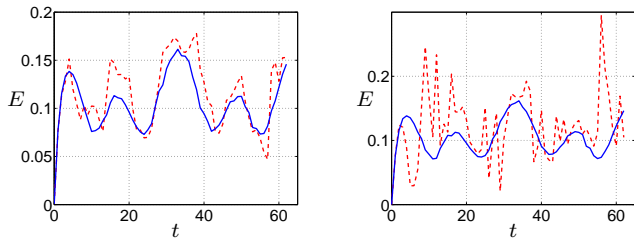


Fig. 4. Evolution of absolute error trajectories with variances of measured noise  $5 \times 10^{-3}$  (left) and  $10^{-1}$  (right).

sensors performs better, the differences between the estimates of the stationary and moving sensors are comparable for variances of order  $10^{-4}$ ,  $10^{-3}$  (the absolute error trajectories overlap) and even not so different when the variances are increased to order  $10^{-2}$ . One has to increase the order of noise to  $10^{-1}$  to observe a clear difference in performance. Qualitatively, Figure 5 shows how the estimated trajectories of the moving sensors (green solid line) behaves compared with the estimation provided by the stationary sensors (black dashed line). The green solid trajectory is very close to the actual trajectory of the target that we do not plot. Note that in all the simulations, the variance of the process noise is kept minimum of order  $10^{-5}$ . It can be observed in the simulations that when the variance of the measurement is kept constant and the variance of the process noise is varied, both performances of stationary and moving sensors give very similar results.

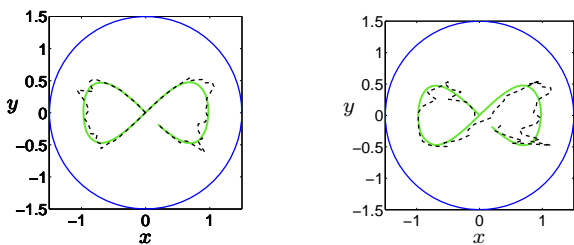


Fig. 5. Qualitative evolution of the estimated trajectories by moving and stationary sensors. Initial positions are  $(0, \pi/2, \pi, 3\pi/2)$  (left) and  $(2.1818, 2.4500, 3.7160, 4.5167)$  (right) and variances are in both cases  $5 \times 10^{-2}$ .

## V. CONCLUSIONS AND FUTURE WORK

We have presented novel decentralized control laws for the optimal positioning of robotic sensor networks that track a target. It would be of clear interest to modify our model by including upper bounds on the motion and detection range

of the sensors. Broader future research lines include (1) heterogeneous collections of sensors, (2) dynamic assignment of sensors to different targets and (3) decentralized estimation and fusion schemes.

## Acknowledgements

This material is based upon work supported in part by ONR YIP Award N00014-03-1-0512 and NSF SENSORS Award IIS-0330008. Sonia Martínez's work was partially supported by a Fulbright Postdoctoral Fellowship from the Spanish Ministry of Education and Culture.

## REFERENCES

- [1] S. Aranda, S. Martínez, and F. Bullo. On optimal sensor placement and motion coordination for target tracking. Technical Report CCEC-04-1013, Center for Control Engineering and Computation. University of California at Santa Barbara, 2004.
- [2] Y. Bar-Shalom, X. R. Li, and T. Kirubarajan. *Estimation with Applications to Tracking and Navigation*. John Wiley, New York, 2001. ISBN 047141655X.
- [3] T. H. Chung, V. Gupta, J. W. Burdick, and R. M. Murray. On a decentralized active sensing strategy using mobile sensor platforms in a network. In *IEEE Conf. on Decision and Control*, pages 1914–1919, Paradise Island, Bahamas, 2004.
- [4] J. Cortés, S. Martínez, T. Karatas, and F. Bullo. Coverage control for mobile sensing networks. *IEEE Transactions on Robotics and Automation*, 20(2):243–255, 2004.
- [5] D. L. Hall and J. Llinas. An introduction to multisensor data fusion. *Proceedings IEEE*, 85(1):6–23, 1997.
- [6] A. Jadbabaie, J. Lin, and A. S. Morse. Coordination of groups of mobile autonomous agents using nearest neighbor rules. *IEEE Transactions on Automatic Control*, 48(6):988–1001, 2003.
- [7] C. S. Kubrusly and H. Malebranche. Sensors and controllers location in distributed systems—a survey. *Automatica*, 21(2):117–128, 1985.
- [8] J. A. Marshall, M. E. Broucke, and B. A. Francis. Formations of vehicles in cyclic pursuit. *IEEE Transactions on Automatic Control*, 49(11):1963–1974, 2004.
- [9] C. D. Meyer. *Matrix Analysis and Applied Linear Algebra*. SIAM, Philadelphia, PA, 2001. ISBN 0898714540.
- [10] A. G. O. Mutambara. *Decentralized Estimation and Control for Multisensor Systems*. CRC Press, Boca Raton, FL, 1998. ISBN 0849318653.
- [11] B. Porat and A. Nehorai. Localizing vapor-emitting sources by moving sensors. *IEEE Transactions on Signal Processing*, 44(4):1018–1021, 1996.
- [12] B. S. Y. Rao, H. F. Durrant-Whyte, and J. S. Sheen. A fully decentralized multi-sensor system for tracking and surveillance. *International Journal of Robotics Research*, 12(1):20–44, 1993.
- [13] B. Sinopoli, L. Schenato, M. Franceschetti, K. Poolla, M. I. Jordan, and S. S. Sastry. Kalman filtering with intermittent observations. *IEEE Transactions on Automatic Control*, 49(9):1453–63, 2004.
- [14] D. Uciński. *Optimal Measurement Methods for Distributed Parameter System Identification*. CRC Press, Boca Raton, FL, 2004. ISBN 0849323134.